Hadron Collider Physics Symposium (HCP2008), Galena, Illinois, USA

# QCD, Tevatron results and LHC prospects

V. Daniel Elvira for the DØ and CDF Collaborations
*FNAL, Batavia, IL 60510, USA*

arXiv:0808.0901v1 [hep-ex] 6 Aug 2008

We present a summary of the most recent measurements relevant to Quantum Chromodynamics (QCD) delivered by the DØ and CDF Tevatron experiments by May 2008. CDF and DØ are moving toward precision measurements of QCD based on data samples in excess of 1 fb$^{-1}$. The inclusive jet cross sections have been extended to forward rapidity regions and measured with unprecedented precision following improvements in the jet energy calibration. Results on dijet mass distributions, $b\overline{b}$ dijet production using tracker based triggers, underlying event in dijet and Drell-Yan samples, inclusive photon and diphoton cross sections complete the list of measurements included in this paper. Good agreement with pQCD within errors is observed for jet production measurements. An improved and consistent theoretical description is needed for $\gamma$+jets processes. Collisions at the LHC are scheduled for early fall 2008, opening an era of discoveries at the new energy frontier, 5-7 times higher than that of the Tevatron.

## 1. PHYSICS MOTIVATION

The last couple of years were filled with excitement at Fermilab. The Tevatron $p\overline{p}$ collider has operated at a center-of-mass energy of 1.96 TeV since 2001, a little less than 10% higher than in the 1991-1995 first period of data taking. In Run 2, the Tevatron reached a peak luminosity of $2.85\times10^{32}$ cm$^{-2}$sec$^{-1}$, delivering more than 4 fb$^{-1}$, almost thirty times more data than collected in Run I. By the end of 2009, the expectation is to accumulate 6-8 fb$^{-1}$ of data. This paper includes a summary of the most recent experimental measurements relevant to Quantum Chromodynamics (QCD) delivered by the DØ and CDF Collaborations by May 2008.

The measurement of the differential inclusive jet and dijet mass cross sections in hadron collisions provides a direct test of perturbative quantum chromodynamics (pQCD). The high $p_T$ range is directly sensitive to the strong coupling constant ($\alpha_s$) and the parton distribution functions (PDFs) of the proton. Deviations from pQCD predictions at large $p_T$ may indicate new physical phenomena not described by the standard model.

The underlying event (UE) is formed by the "beam-beam remnants" from the breakup of the proton and antiproton. Experimentally, in a dijet sample, the UE is typically defined as everything in the event except the two outgoing hard scattered jets, and consists of the beam-beam remnants plus initial and final-state radiation. An accurate measurement of the UE is important to, for example, understand particle (hadron) level measurements of jet cross sections compared with parton and hadron level theoretical predictions. The UE will be an important element of the hadronic environment at the LHC, affecting all processes from Higgs searches to physics beyond the standard model. It is therefore important to construct models to predict the UE at the LHC energies, based on the data currently available.

The production of a photon with associated jets in the final state is a powerful probe of the dynamics of hard QCD interactions. Different angular configurations between the photon and the jets can be used to extend inclusive photon production measurements and simultaneously test the underlying dynamics of QCD hard-scattering subprocesses in different regions of parton momentum fraction $x$ and large hard-scattering scales $Q^2$. Diphoton final states are a signature of many interesting physics processes. The understanding of the QCD production mechanism is therefore a pre-requisite to a reliable search. For example, at the LHC, one of the main decay channels for the Higgs boson would be the $\gamma\gamma$ final state. An excess production of $\gamma\gamma$ at high invariant mass could be a signature of large extra dimensions. In many theories involving physics beyond the standard model, cascade decays of heavy new particles generate a $\gamma\gamma$ signature.

## 2. SAMPLE SELECTION AND CORRECTIONS

The DØ and CDF detectors are described elsewhere [1, 2].

### 2.1. Jets

The primary tool for jet detection in both DØ and CDF is the calorimeter system which provides good electron and hadron energy resolution, a fine segmentation, hermeticity, and shower containment. The tracker system plays a fundamental role in identifying the secondary vertex in the case of the b-jet cross section measurement.

For the analyses shown in these proceedings, the Run II iterative seed-based cone jet algorithm including mid-points [3] (Midpoint algorithm) with cone radius 0.7 in rapidity $y$ and azimuthal angle is used to cluster energies deposited in calorimeter towers. The same algorithm is used for partons in the pQCD calculations.

Cosmic rays and beam related backgrounds are removed by applying loose cuts on the ratio of the event missing transverse energy ($\not\!\!E_T$) and the leading jet $E_T$ (DØ ), or on the $\not\!\!E_T$ significance (CDF). Requirements on characteristics of shower development for genuine jets are used to remove the remaining background due to electrons, photons, and detector noise that mimic jets.

The jet $p_T$ is corrected for the energy response of the calorimeter, energy showering in and out the jet cone, and additional energy from event pile-up and multiple proton interactions [4, 5]. The jet energy corrections fix the calorimeter jet four-momentum to the particle (hadron) level energy. The electromagnetic part of the calorimeter is calibrated using $Z \to e^+e^-$. The $\eta$-dependence of the jet response is determined using event $p_T$ balance in dijet events. At DØ the $p_T$-dependent absolute correction is derived from event $p_T$ balance in $\gamma$-jet events. Further corrections due to the difference in response between quark- and gluon-initiated jets are computed using the PYTHIA[6] event generator, passed through a geant-based [7] simulation of the detector response. In CDF, the absolute correction is derived from Monte Carlo events, based on the GEANT3 [7] detector simulation tool kit, in which a parameterized shower simulation, GFLASH [8], is used to model the energy deposited in the calorimeter. The GFLASH parameters are tuned to test-beam data for electrons, and high momentum charged pions and the in-situ collision data for electrons from Z decays and low-momentum charged hadrons. The fractional uncertainty of the jet $p_T$ calibration is less than 2(3)% for DØ (CDF) in the kinematic range covered in the measurements.

Jet cross sections are unfolded to correct for the effect of finite energy resolution using a four-parameter ansatz function to parameterize the $p_T$ dependence (DØ ), or a smeared PYTHIA distribution weighted to match the data (CDF) [4, 5].

#### 2.1.1. b-jets

Jets initiated by b-quarks are selected in CDF using a trigger based on two jets with $p_T$ >20 GeV associated with two displaced tracks reconstructed using the Silicon Vertex Trigger (SVT) system. Offline, jets are tagged using an algorithm based on the reconstruction of a secondary vertex inside the jet, and a requirement for the impact parameter to be >120 $\mu$m. An SVT b-tagged jet is defined so that events with two such objects always pass the trigger. The efficiency for requiring two SVT b-tagged jets in an event is calculated from a Monte Carlo simulation. The shape of the invariant mass of the tracks associated to the secondary vertex can be used to separate the contribution of heavy flavor jets from light quark and gluon jets. A two components fit to the data is performed, based on Monte Carlo templates. A "signal" template describes the $b\overline{b}$ case and a "background" template all the other possible contributions.

### 2.2. Photons

The DØ experiment selects photon candidates from clusters of calorimeter cells within a cone of radius R=0.4 defined around a seed tower [1, 9, 10]. The final cluster energy is then re-calculated from the inner cone with R=0.2. The selected clusters are required to have greater than 96% of their total energy contained in the EM calorimeter

layers. Isolated clusters are selected by requiring the energy outside an R=0.2 cone to be a small fraction of the photon energy. The candidate EM cluster is required not to be spatially matched to a reconstructed track. This is accomplished by computing a $\chi^2$ function evaluating the consistency, within uncertainties, between the reconstructed $\eta$ and $\phi$ positions of the cluster and the closest track measured in the layer located at the shower maximum position. The corresponding $\chi^2$ probability is required to be <0.1%. Background contributions to the direct photon sample from cosmic rays and from isolated electrons, originating from the leptonic decays of $W$ bosons, important at high $p_T^\gamma$, are suppressed with a cut on $\not{E}_T$. Photons arising from decays of $\pi^0$ and $\eta$ mesons are already largely suppressed by the requirements above, and especially by photon isolation. The position and width of the Z boson mass peak, reconstructed from $Z \to e^+e^-$ events, are used to determine the EM calorimeter calibration factors and the EM energy resolution. The CDF experiment uses a very similar selection criteria, described in Ref. [11].

## 3. JET CROSS SECTIONS

### 3.1. Inclusive Jet Measurements

The DØ inclusive jet cross section measurements corrected to particle (hadron) level are performed in six $|\eta|$ bins as a function of $p_T$ . The cross section corresponds to an L=0.7 pb$^{-1}$ sample, extending over more than eight orders of magnitude from $p_T$= 50 GeV to $p_T$ > 600 GeV. Perturbative QCD predictions to next-to-leading order (NLO) in $\alpha_s$, computed using the fastNLO program [12] (based on nlojet++ [13]) and the PDFs from CTEQ6.5M [14], are compared to the data. The predictions are corrected for non-perturbative contributions due to the underlying event and hadronization computed by pythia with the CTEQ6.5MPDFs, the QWtune [15], and the two-loop formula for $\alpha_s$. The ratio of the data to the theory is shown in Fig. 1. The dashed lines show the uncertainties due to the different PDFs coming from the CTEQ6.5 parameterizations. The predictions from MRST2004 [16] are displayed by the dotted line. In all $y$ regions, the predictions agree well with the data. There is a tendency for the data to be lower than the central CTEQ prediction, particularly at very large $p_T$, but the results are mostly within the CTEQ PDF uncertainty band. The $p_T$ dependence of the data is well reproduced by the MRST parameterization. The point-to-point correlations for the 24 different sources of systematic uncertainties are given in Ref. [17].

CDF measured the inclusive differential jet cross sections as a function of $p_T$ and rapidity, corrected to the hadron level. The data-to-theory ratios, based on NLO pQCD predictions from fastNLO [12], are shown in Fig. 2. The measured inclusive jet cross sections tend to be lower but still in agreement with the NLO pQCD predictions. To quantify the comparisons, a procedure based on a $\chi^2$ test was performed which included information on individual systematic uncertainties and their correlations, as well as different choices in the theory calculation. This test yielded agreement probabilities of 71, 91, 23, 69, and 91% when performed separately in the five rapidity regions. CDF also measured the inclusive jet cross sections with a $k_T$ algorithm. Reasonable agreement of the ratio of the $k_T$ and Midpoint cone results is reported in Ref. [5].

### 3.2. Dijet Mass Measurements

A preliminary CDF dijet mass cross section measurement for jets with $|\eta|$ <1 in a 1.13 pb$^{-1}$ sample is compared in Fig. 3 to the NLO pQCD predictions from fastNLO[12, 13]. For the PDF in the proton, CTEQ6.1 is used, and the renormalization and factorization scales are set to the average $p_T$ of the leading two jets. The NLO pQCD predictions for jets of partons are corrected for the non-perturbative underlying and hadronization effects. These are derived by running the jet clustering algorithm to the hadron on parton and hadron level events generated with PYTHIA. Good agreement between data and theory is observed to within the uncertainties in the measurement and the prediction. An important motivation for this measurement is the search for new physics, which would show as deviations of the data with respect to the QCD predictions. Limits could be set, for example, to excited quark, massive gluon, $Z'$ and $W'$ production. We will not discuss searches in these proceedings.

### 3.3. $b\bar{b}$ Dijet Measurement

The CDF preliminary $b\bar{b}$ dijet cross section using the SVT is based on a 260 pb$^{-1}$ sample. Figures 4, 5 show the cross section for $b\bar{b}$ dijet production as a function of the invariant mass and the separation in azimuthal angle of the two jets. The measurement is compared to predictions from LO generators such as PYTHIA and HERWIG [18], as well as to NLO predictions from MC@NLO[19], interfaced with the HERWIG parton shower and using a minimum quark $p_T$ of 10 GeV in $|\eta|$ <1.75 and CTEQ6.1M. PYTHIA samples are generated with the "tune A" [20] for the underlying event modeling. JIMMY [21] is used with HERWIG and MC@NLO to include the effect of multiple parton interactions. As illustrated in Figs. 4-5, the agreement between the data and the theory improves as we move from a LO prediction to HERWIG or MC@NLO with JIMMY, which includes multiple parton interactions.

## 4. UNDERLYING EVENT

CDF has released a preliminary measurement of the underlying event based on 2.7 fb$^{-1}$ samples. Although the UE is formally defined as the contributions from the remnants of the colliding beams and multiple parton interactions, it is difficult to separate these contributions from those of initial and final state radiation. The UE is therefore studied from dijet events by measuring all particles except those associated with the two outgoing jets, and from Drell-Yan (DY) events by excluding the two outgoing leptons. In dijet events, "TransMax" and "TransMin" regions, describes the two sectors in $\phi$ perpendicular to the direction of the leading jet. This definition allows to separate the hard from the soft component of the UE; while TransMax is sensitive to both the initial/final state radiation and the beam remnants, TransMin is more sensitive to the beam remnants. In DY events, the "Toward" region is defined in the direction of the di-lepton system originated from the $Z$ boson; the "Transverse" and "Toward" regions are therefore both sensitive to the UE, while the "Away" region contains the hadronic recoil.

CDF measured the scalar $p_T$ sum density of the charged particles in DY events as a function of the transverse momentum of the lepton pair (electron and muon samples combined). While the sum increases with $p_T$ in the Away region due to the contribution of the hadronic recoil, the Toward and Transverse regions show a flat behavior. The comparison of the Transverse regions for DY and dijet data in Fig. 6 shows a similar trend, suggesting universality of the UE in hard scattering processes. The dotted lines are the different PYTHIA tunes which clearly describe the data reasonably well.

## 5. PHOTON PRODUCTION

### 5.1. Inclusive $\gamma$+jets Measurement

DØ has recently performed measurements of the inclusive $\gamma$ and $\gamma$+jet cross sections [9, 10]. The CDF Collaboration has released a preliminary measurement of the inclusive $\gamma$ cross section based on 451 pb$^{-1}$. The $\gamma$+jet+X final state is dominated by compton $qg$ scattering for $p_T \lesssim$120 GeV. The DØ measurement is based on a 1 fb$^{-1}$ sample and probes the gluon density function in the 0.007$\leq X \leq$0.8 range for 900$\leq Q^2 \equiv (p_T^\gamma)^2 \leq$ 1.6$\times$ 10$^5$ GeV$^2$. The trick is achieved by measuring the cross section for different angular configurations between the $\gamma$ and the leading jet: central or forward, positive or negative $y^\gamma$ and $y^{jet}$ as a function of $p_T^\gamma$.

The ratio of the measured cross section to the NLO QCD prediction JETPHOX [22] is taken in each interval and the results are shown in Fig. 7. The data-to-theory ratios have a shape similar to those observed in the inclusive photon cross sections measured by the UA2, CDF and DØ collaborations. Different choices of PDFs or parameters in the theory are not able to simultaneously accommodate the measured differential cross sections in all of the regions.

A more precise measurement can be performed by taking the ratios of cross sections for different configurations, for which most of the systematic uncertainties cancel, leaving a residual 3-9% error across most of the $p_T$ domain. These ratios, shown in Fig. 8, are qualitatively reproduced by the theory. A quantitative difference, however, is observed

for the ratios of the central jet regions to the forward 1.5< $|y^{jet}|$ <2.5, $|y^{jet}| > 0$ region, even after the theoretical scale variation is taken into account.

## 5.2. Diphoton Measurement

A result which is unique to CDF is the measurement of diphoton distributions. The two dominant contributions to diphoton production come from the LO $q\overline{q}$ process which is dominant at high mass and the NLO $gg$ process which, in spite of being suppressed by $\alpha_s^2$ with respect to the $q\overline{q}$ diagram, is still relevant at low mass. The measurement is based on a 207 pb$^{-1}$ sample, with 889 diphoton candidate events surviving the selection requirements. Results are compared to the LO PYTHIA calculation, the DIPHOX [23] NLO prediction, which includes the $gg$ process, and RESBOS [24], a NLO calculation which resums the effects of initial state soft gluon radiation but includes only LO fragmentation contributions. Figures 9, 10 show the diphoton cross sections as a function of the photon $q_T$ and $\Delta\phi_{\gamma\gamma}$. It is apparent that the data favors the RESBOS calculation at low $q_T$ and $\Delta\phi_{\gamma\gamma}$ greater than $\phi/2$, where initial state gluon radiation is important. By contrast, in the region where fragmentation becomes relevant, large $q_T$ and $\Delta\phi_{\gamma\gamma} < \pi/2$, DIPHOX does a better job. For agreement in all areas, a resummed full NLO calculation would be necessary.

## 6. SUMMARY AND LHC PROSPECTS

The Tevatron experiments are entering an era of precision QCD measurements based on samples in excess of 1 fb$^{-1}$. Good agreement with pQCD within errors is observed for jet production measurements. An improved and consistent theoretical description is needed for $\gamma$+jets. Collisions at the LHC are scheduled for early fall 2008, opening an era of discoveries at the new energy frontier, 5-7 times higher than that of the Tevatron.

## References


[1] V. M. Abazov *et al.* (DØ Collaboration), Nucl. Instrum. Methods A 565, 463 (2006).
[2] D. Acosta *et al.* (CDF Collaboration), Phys. Rev. D 71, 052003 (2005).
[3] G.C. Blazey *et al.*, in Proceedings of the Workshop: "QCD and Weak Boson Physics in Run II", edited by U. Baur, R. K. Ellis, and D. Zeppenfeld, Batavia, Illinois (2000) p. 47.
[4] V. M. Abazov *et al.*, Accepted by Phys. Rev. Lett., 0802.2400 [hep-ex] (2008).
[5] T. Aaltonen *et al.* (CDF Collaboration), Submitted to Phys. Rev. D arXiv:0807.2204v1 [hep-ex] (2008).
[6] T. Sjöstrand *et al.*, Comp. Phys. Comm. 135, 238 (2001).
[7] R. Brun and F. Carminati, CERN Program Library Long Writeup W5013, 1993 (unpublished).
[8] G. Grindhammer, M. Rudowicz, and S. Peters, Nucl. Instrum. Methods Phys. Res., Sect. A 290, 469 (1990).
[9] V. M. Abazov *et al.* (DØ Collaboration), Phys. Lett. B 639, 151 (2006).
[10] V. M. Abazov *et al.* (DØ Collaboration), Submitted to Phys. Lett. B, arXiv:0804.1107 [hep-ex] (2008).
[11] D. Acosta *et al.* (CDF Collaboration), Phys. Rev. Lett. 95, 022003 (2005).
[12] T. Kluge, K. Rabbertz, M. Wobisch, arXiv:hepph/0609285.
[13] Z. Nagy, Phys. Rev. D 68, 094002 (2003).
[14] W. K. Tung *et al.*, JHEP 0702, 053 (2007); J. Pumplin *et al.*, JHEP 0207, 12 (2002); D. Stump *et al.*, JHEP 0310, 046 (2003).
[15] R. Field, M. G. Albrow *et al.* [TeV4LHC QCDWorking Group], arXiv:hep-ph/0610012.
[16] A. D. Martin *et al.*, Phys. Lett. B 604, 61 (2004).
[17] Measurements and correlations are available at HTTP://WWW-D0.FNAL.GOV /RUN2PHYSICS/WWW/RESULTS/FINAL/QCD/Q08A/.
[18] G. Corcella *et al.*, HERWIG 6, JHEP 01, 10 (2001).

[19] S. Frixione, B. R. Webber, JHEP 0206 (2002).
[20] T. Affolder *et al.*, Phys. Rev. D 65, 092002 (2002).
[21] J. M. Butterworth, J. R. Forshaw, M. H. Seymour, Multi-parton interactions in photoproduction at HERA.
[22] S. Catani *et al.*, JHEP 05, 028 (2002).
[23] T. Binoth, J. Ph. Guillet, E. Pilon, and M. Werlen, Eur. Phys. J. C 16, 311 (2000).
[24] C. Balazs, E. L. Berger, S. Mrenna, and C. -P. Yuan, Phys. Rev. D 57, 6934 (1998).

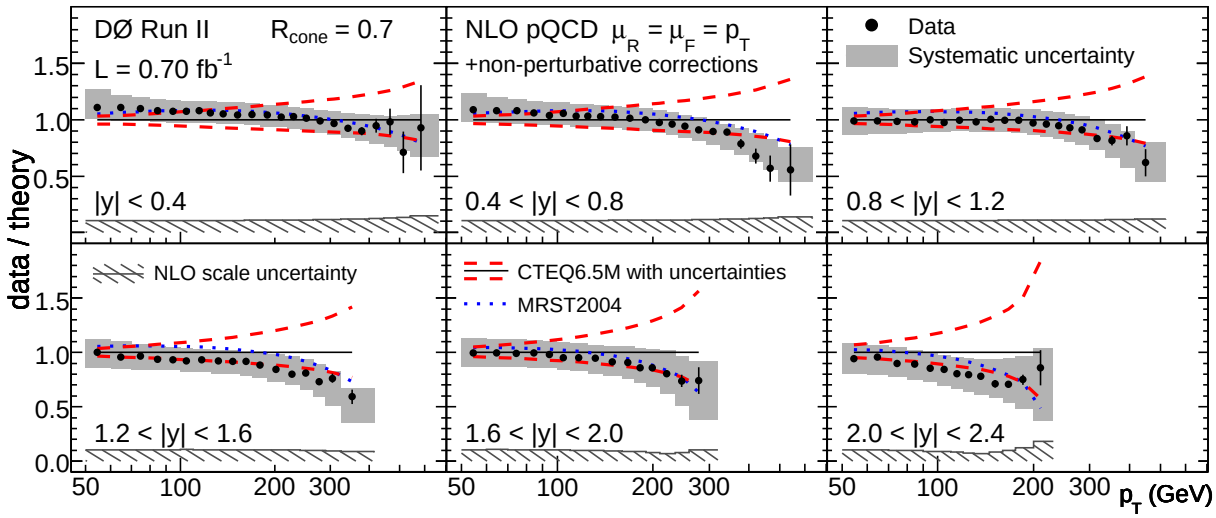


Figure 1: Measured data-to-theory ratio for the inclusive jet cross section as a function of jet $p_T$ in six $|y|$ bins. The data systematic uncertainties are displayed by the full shaded band.

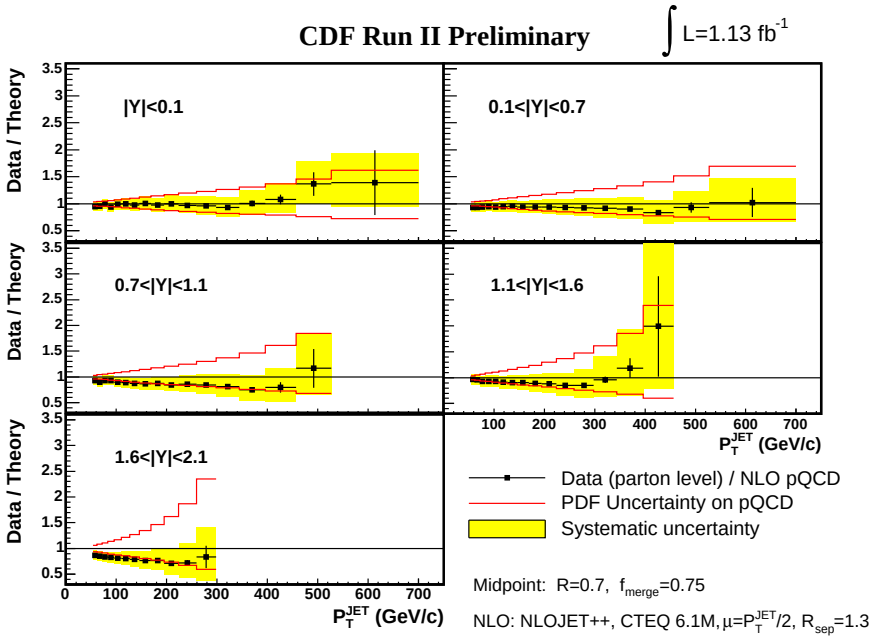


Figure 2: Measured data-to-theory ratio for the inclusive jet cross section as a function of jet $p_T$ in six $|y|$ bins. The data systematic uncertainties are displayed by the full shaded band.

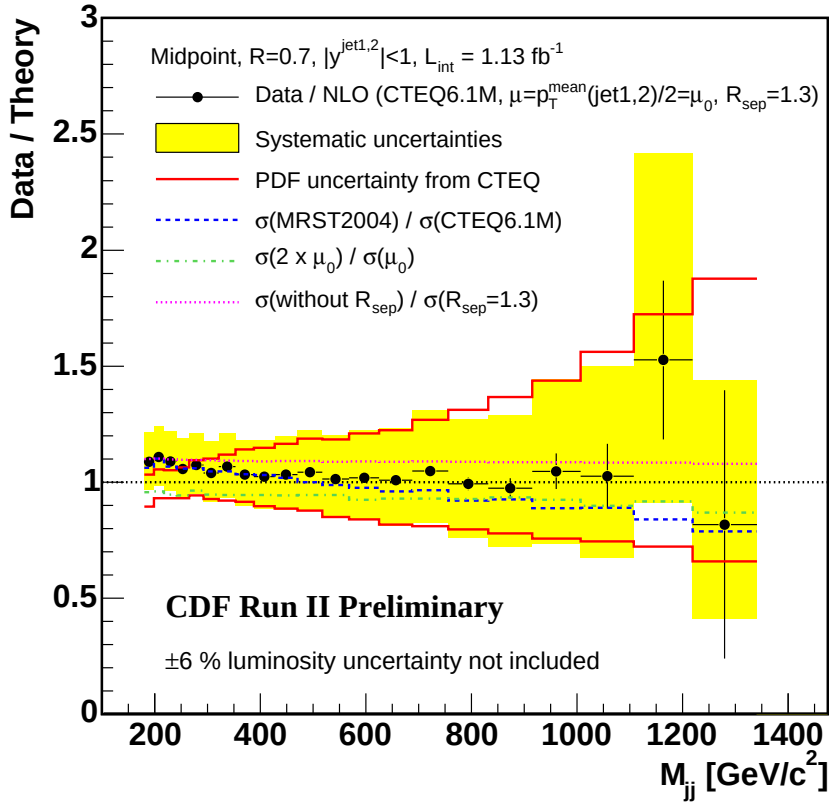


Figure 3: The ratio of the CDF preliminary dijet mass cross section to NLO pQCD predictions, including the systematic error band of the measurement, and the theory uncertainty from the choice of PDFs.

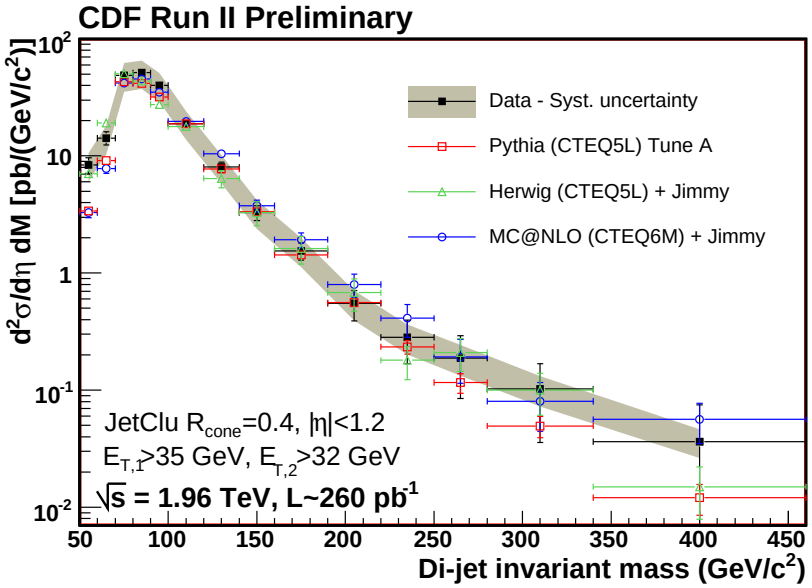


Figure 4: Cross section for $b\bar{b}$ dijet production as a function of the invariant mass of the two jets.

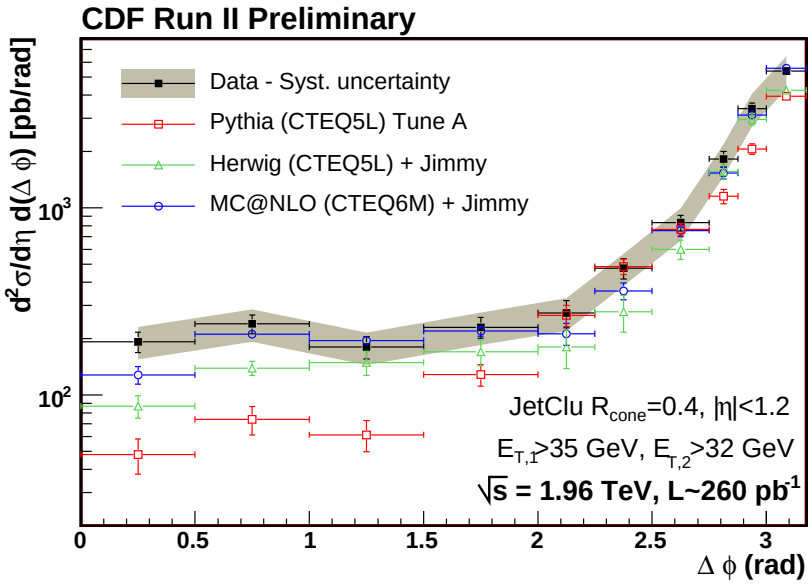


Figure 5: Cross section for $b\bar{b}$ dijet production as a function of the separation in azimuthal angle between the two jets.

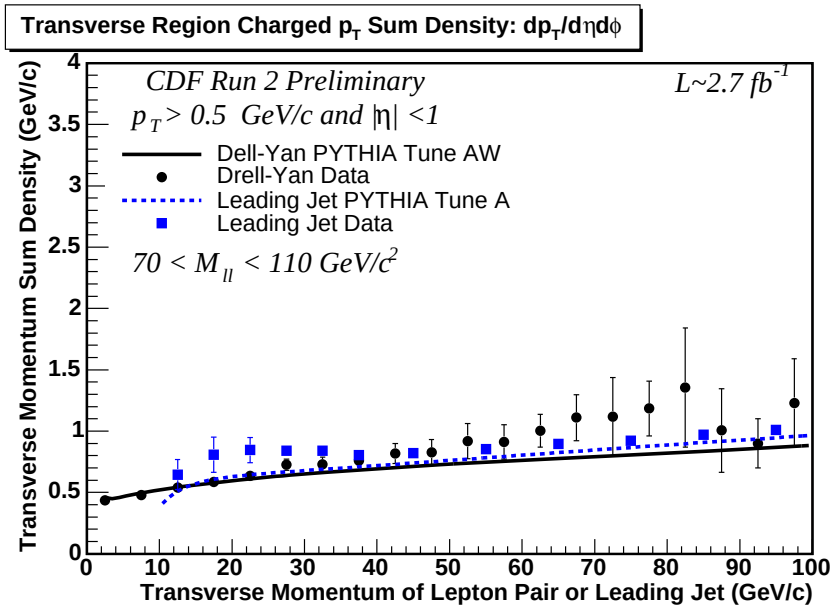


Figure 6: Transverse momentum sum density as a function of the $p_T$ of either the lepton pair or the leading jet. The results from the dijet and the combined electron/muon sample are compared. The error bars include both the statistical and systematic uncertainties.

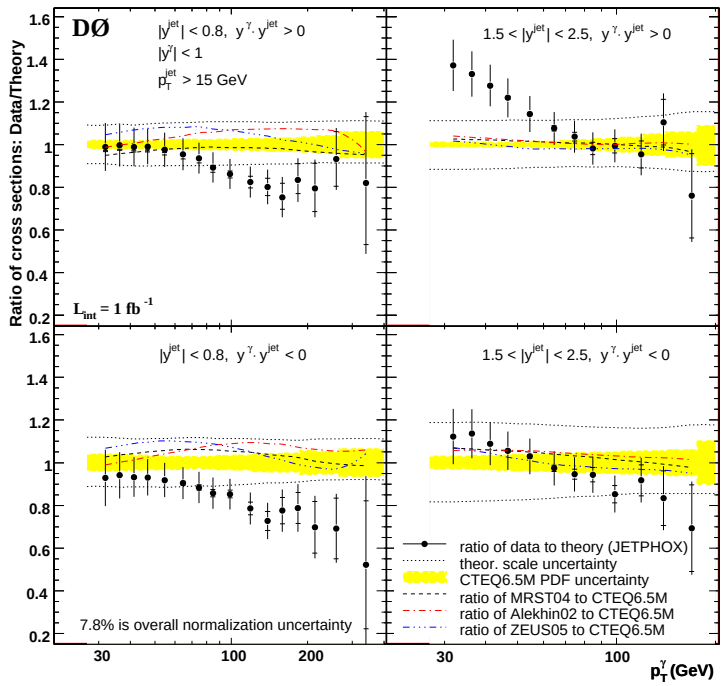


Figure 7: The ratios of the measured cross section, in each measured interval, to the NLO QCD prediction using JETPHOX with the CTEQ6.5M PDF set.

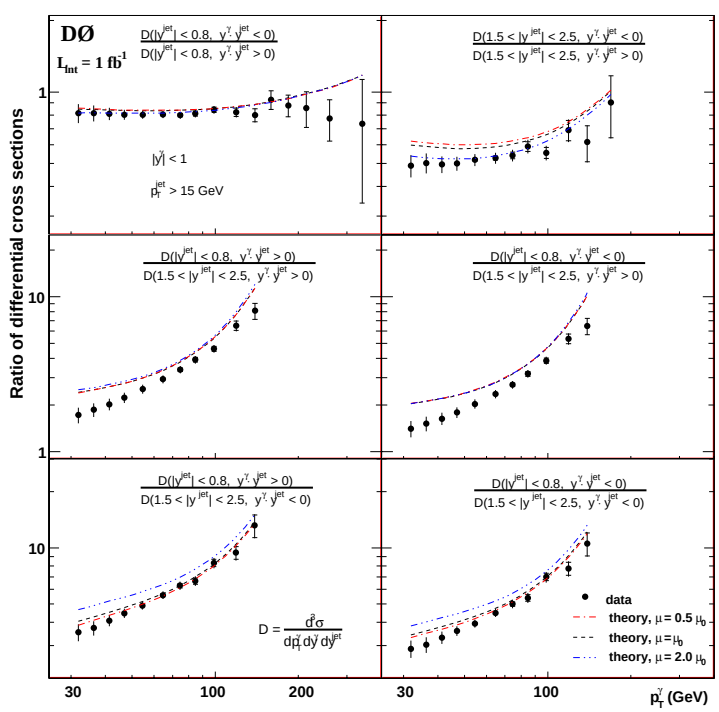


Figure 8: The ratios between the cross sections in each $|y^{jet}|$ region. The solid vertical error bars correspond to the statistical and systematic uncertainties added in quadrature while the horizontal marks indicate the statistical uncertainty. NLO QCD theoretical predictions for the ratios are estimated using JETPHOX.

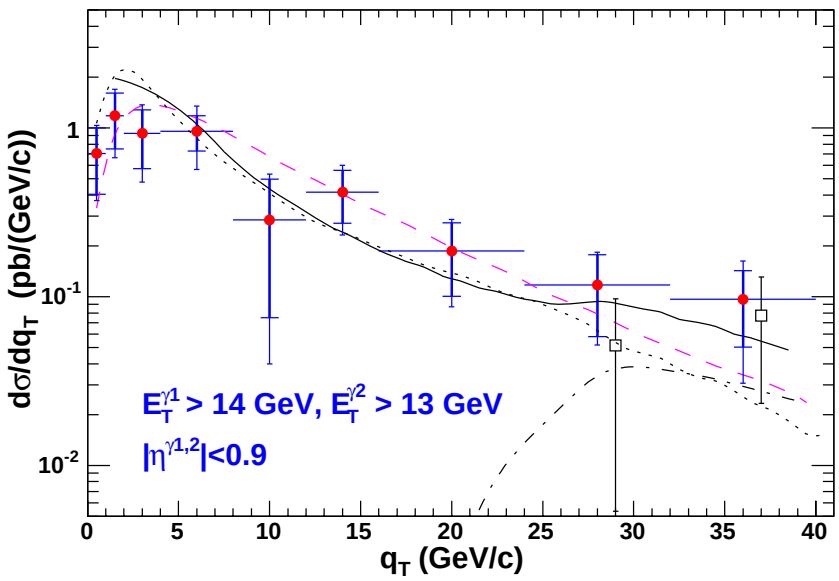


Figure 9: The $\gamma\gamma$ $q_T$ distribution from the CDF Run II data, along with predictions from DIPHOX (solid line), RESBOS (dashed line), and PYTHIA (dot-dashed line).

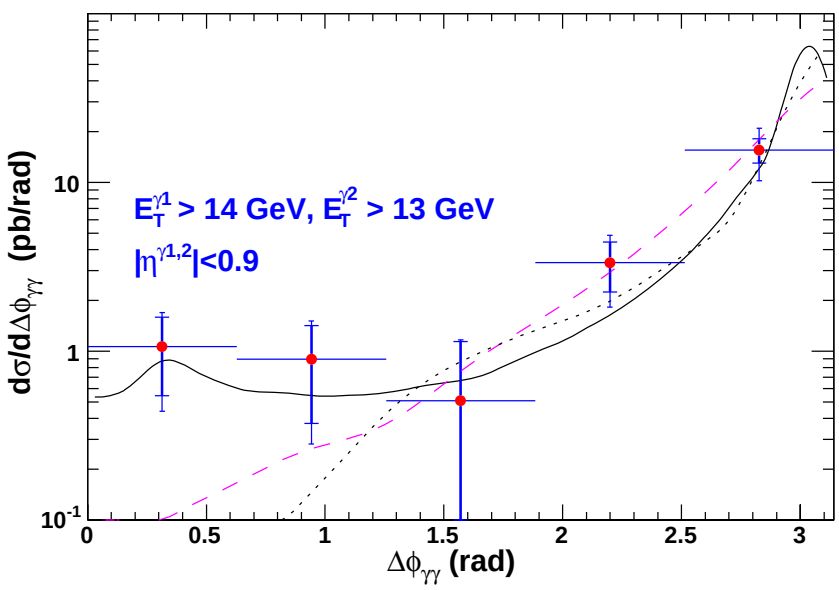


Figure 10: The $\gamma\gamma$ $\Delta\phi_{\gamma\gamma}$ angular distribution from the CDF Run II data, along with predictions from DIPHOX (solid line), RESBOS (dashed line), and PYTHIA (dot-dashed line).